Validation of 4-[Fluorine-18]Fluoro-3-Iodobenzylguanidine as a Positron-Emitting Analog of MIBG

Ganesan Vaidyanathan, Donna J. Affleck and Michael R. Zalutsky

Department of Radiology, Duke University Medical Center, Durham, North Carolina

This study evaluates the potential utility of 4-[^{18}F]fluoro-3-iodobenzylguanidine ([^{18}F]FIBG) as an MIBG analog. **Methods:** In vitro assays of tracer binding were carried out using the SK-N-SH human neuroblastoma cell line in a paired-label format to compare [^{18}F]FIBG directly with no-carrier-added [^{125}I]MIBG. To ascertain whether [^{18}F]FIBG, like MIBG, is taken up by the uptake-1 mechanism, the effects of desipramine, norepinephrine, and carrier MIBG and FIBG on cell binding were determined. Preincubation with ouabain and incubation at 4°C was used to evaluate the energy-dependence of [^{18}F]FIBG uptake by SK-N-SH cells. The tissue distribution of [^{18}F]FIBG in mice was compared with no-carrier-added [^{125}I]MIBG in a paired-label study. **Results:** In paired-label binding studies, the percent binding of [^{18}F]FIBG to neuroblastoma cells remained constant over a three-log activity range and the level was somewhat higher than that of no-carrier-added [^{125}I]MIBG. Binding was blocked by desipramine, norepinephrine, carrier MIBG and FIBG, ouabain and by incubating at 4°C, suggesting that [^{18}F]FIBG is taken up by the uptake-1 mechanism. Radiation dosimetry calculations suggest that higher doses of [^{18}F]FIBG, unlike [^{124}I]MIBG, could be administered to patients. **Conclusion:** These in vitro and in vivo evaluations show that [^{18}F]FIBG is an excellent analog of MIBG, suggesting that [^{18}F]FIBG should be further evaluated for use in PET imaging of neuroendocrine tumors and cardiac abnormalities.

Key Words: fluorine-18; neuroendocrine tumors; positron emission tomography; metaiodobenzylguanidine; cardiac abnormalities

J Nucl Med 1995; 36:644–650

Metaiodobenzylguanidine (MIBG) is a functional analog of the neurotransmitter norepinephrine. It is transported, stored and released by a mechanism similar to that of norepinephrine (*1,2*). Since myocardial norepinephrine concentration is altered by a number of pathological conditions (*3*), radioiodinated MIBG has found use in the scintigraphic evaluation of conditions such as cardiomyopathy (*4*) and myocardial infarction (*5*). MIBG has also been used for the localization and therapy of neuroendocrine tumors such as pheochromocytoma and neuroblastoma (*6,7*).

In imaging, both planar scintigraphy and SPECT have been used in combination with [^{131}I/^{123}I]MIBG (*8,9*). Use of planar scintigraphy and/or SPECT in combination with [^{123}I]MIBG has been reported to improve lesion detection compared to planar scintigraphy using [^{131}I]MIBG. For example, Shuklin et al. (*10*) were able to detect a lesion in a patient with strong clinical and laboratory evidence for pheochromocytoma using [^{123}I]MIBG and SPECT but not with planar imaging and [^{131}I]MIBG. The sensitivity of [^{123}I]MIBG over that of [^{131}I]MIBG, especially in the detection of metastasis, has also been documented (*11*). A number of groups have been interested in extending this approach by applying PET, which like SPECT, offers the advantage of tomographic imaging, but can provide more rigorous attenuation correction, resulting in superior quantitative capabilities.

From a validation standpoint, [^{124}I]MIBG would be advantageous for PET because the pharmacokinetics and uptake-1 mechanism of this tracer would be expected to be identical to those observed with other radioiodinated MIBG compounds. The ability to perform PET imaging using [^{124}I]MIBG has been demonstrated (*12*). Use of ^{124}I-labeled compounds, however, has been confined to only a few centers because of the general lack of availability of this nuclide. In addition, its 4.2 day half-life is not ideally matched with the biokinetics of MIBG. The relatively long half-life of ^{124}I, coupled with the presence of multiple high energy gamma rays in its decay scheme, could limit the dose administered for diagnostic applications.

With regard to other PET labels, the Orsay group synthesized meta-[^{76}Br]bromobenzylguanidine ([^{76}Br]MBBG) and reported that this tracer behaves in similar fashion to MIBG (*13,14*). Widespread application of this tracer may be hindered by the limited availability of ^{76}Br and the high energy of its positron emissions. Because ^{18}F is the longest-lived positron-emitting nuclide routinely available at most PET centers, we have been interested in the development of an MIBG analog labeled with ^{18}F. As an initial approach, para- and meta-[^{18}F]fluorobenzylguanidine were

Received May 16, 1994; revision accepted Sept. 13, 1994.

For correspondence or reprints contact: Ganesan Vaidyanathan, PhD, Box 3808, Department of Radiology, Duke University Medical Center, Durham, NC 27710.

investigated (*15*). Binding to neuroblastoma cells in vitro and localization in the heart and adrenals in vivo could be demonstrated, albeit, at significantly lower levels than observed with MIBG.

Hypothesizing that fluoro for iodo substitution had altered the behavior of fluorobenzylguanidine as a consequence of decreased lipophilicity, we developed a no-carrier-added synthesis of 4-[^{18}F]fluoro-3-iodobenzylguanidine, [^{18}F]FIBG (*16*). Preliminary results suggested that this compound might be a useful analog of MIBG for use in PET. In the current study, we present further evaluations of the clinical potential of [^{18}F]FIBG. The results of in vitro binding experiments, paired-label biodistribution measurements and dosimetry calculations suggest that [^{18}F]FIBG exhibits a similar uptake mechanism and tissue distribution pattern as MIBG and has acceptable dosimetry for administration to patients.

MATERIALS AND METHODS

Desipramine (DMI) and norepinephrine (arterenol) were obtained from Sigma. Sodium [^{125}I]iodide in 0.1 N NaOH was supplied by DuPont-New England Nuclear (N. Billerica, MA).

No-carrier-added Iodine-125-MIBG

This agent was prepared using an identical procedure reported for the preparation of the ^{131}I and ^{123}I analogs (*17,18*). Briefly, a solution of N-chlorosuccinimide in trifluoroacetic acid (0.3 *M*; 10 μl) was added to 1–2 mCi of [^{125}I]iodide (2–3 μl) in a Reacti® vial followed by a solution of N-chlorosuccinimide in trifluoroacetic acid (0.3 *M*; 10 μl) followed by a solution of the silicon precursor, 3-trimethylsilylbenzylguanidine in trifluoroacetic acid (0.1–0.15 *M*; 5 μl). The mixture was vortexed and left at room temperature for 5 min. Iodine-125-MIBG was isolated/purified by reverse-phase HPLC using a Waters μ Bondapak C18 (10 μm, 3.9 × 300 mm) column eluted with water:tetrahydrofuran:triethylamine: phosphoric acid (96.5:2.0:1.0:0.5 v/v/v/v) at 3 ml/min. The radiochemical yield was more than 90%. Use of a C18 solid-phase cartridge facilitated desalting and reconstitution of the activity from the HPLC fractions into the appropriate buffers for in vitro and in vivo experiments. The specific activity was at least 1200 Ci per mmole.

No-carrier-added Fluorine-18-FIBG

This compound was synthesized as previously reported (*16*). Briefly, 4-cyano-2-iodo-(N,N,N-trimethyl)anilinium trifluoromethanesulfonate was radiofluorinated using [^{18}F]KF and Kryptofix® in DMSO. The resultant 4-[^{18}F]fluoro-3-iodobenzonitrile was reduced using $NaBH_4/I_2$. The 4-[^{18}F]fluoro-3-iodobenzylamine thus produced was converted to [^{18}F]FIBG, first by treating it with N,N'-(di-tert-butyloxycarbonyl)thiourea in the presence of mercuric chloride and triethylamine in DMF, and then deprotecting the intermediate with trifluoroacetic acid. The final product (in 5% overall decay corrected yield) was purified by reverse-phase HPLC using a Waters μ Bondapak C18 (10 μm, 3.9 × 300 mm) column eluted with 0.2 *M* ammonium phosphate:tetrahydrofuran (80:20 v/v) at 0.8 ml/min. Desalting and reconstitution was performed as with [^{125}I]MIBG. The specific activity was more than 1500 Ci/mmole.

Cell Lines

The human neuroblastoma cell lines SK-N-SH and SK-N-MC (*19*) were purchased from American Type Culture Collection (Rockville, MD). The SK-N-SH line was used as the target (*20*) and SK-N-MC line as a negative control. Previous experiments have demonstrated the lack of binding of MIBG to the SK-N-MC lines (*17*). The incubation medium (JRH Biosciences, Lenexa, KS) was made by mixing 440 ml of RPMI 1640, 50 ml of Serum Plus, 5 ml of penicillin-G/streptomycin (5000 U of penicillin and 5000 μg of streptomycin in 1 ml) and 5 ml of glutamine (200 m*M* in saline). The cells were grown at 37°C in a humidified incubator with 5% CO_2.

Binding of Fluorine-18-FIBG to SK-N-SH Human Neuroblastoma Cells

The cells were seeded into 24-well plates (4 × 10^5 cells in 500 μl medium/well) and incubated for 24 hr in a 37°C/5% CO_2-humidified atmosphere. For mechanistic studies, the cells were preincubated with various interventional agents for 30 min at 37°C before adding the tracer. Cells were then incubated with [^{18}F]FIBG for 2 hr at 37°C. To determine the effect of temperature on uptake, additional experiments were carried out using incubations at 4°C for 2 hr. Some experiments were performed in a paired-label format by coincubating no-carrier-added [^{125}I]MIBG with [^{18}F]FIBG to determine whether the concentration of halobenzylguanidines (or impurities) in the two preparations, if present, were sufficient to inhibit cell binding. In some cases, the uptake of individual tracers was also determined in parallel. For dose-dependence studies, 7.5 nCi–750 nCi of each tracer were used. For mechanistic studies, about 250 nCi of each tracer were used. To determine nonspecific binding, we measured either the binding to SK-N-SH cells in the presence of 50 μ*M* DMI or the binding to the negative control SK-N-MC line. In all experiments, the medium was removed at the end of the 2-hr incubation and the cells were washed twice with phosphate-buffered saline. The cells were solubilized by incubation with 500 μl of 0.5 N NaOH for 30 min at room temperature and then removed with cotton swabs. The cell bound activity was counted along with input standards using an automated gamma counter. The results were expressed as the percent of input activity bound to the cells. Each measurement was performed in triplicate or quadruplicate.

Tissue Distribution in Mice

Two studies were conducted using BALB/c mice. In the first, the tissue distribution was performed in a paired-label format by coinjecting mice (25 g–28 g) with 2 or 3 μCi each of [^{18}F]FIBG and no-carrier-added [^{125}I]MIBG. The tissue distribution was determined at 1 and 2 hr postinjection. The tissue uptake of each tracer was also determined individually (single-label) at 2 hr to determine the validity of using paired-label format (i.e., whether the combined mass of the two tracers was sufficient to alter biodistribution). In the second study, the effect of desipramine on the tissue uptake, especially in heart and adrenals, was determined. A group of five mice (26–28 g) was injected intraperitonially with 0.25 mg (~10 mg/kg) of desipramine in 100 μl of phosphate-buffered saline 30 min before tracer administration. The control group received just the saline vehicle. Subsequently, both groups were administered 4 μCi of [^{18}F]FIBG. Tissue uptake was determined 1 hr postinjection. In both studies, the mice were killed by halothane overdose, dissected and the tissues of interest were isolated. The tissues were washed with saline, blot-dried, weighed and counted in a gamma counter for ^{18}F and/or ^{125}I activity. The results were expressed as %ID/g, the percentage of injected dose per gram of tissue.

Radiation Dosimetry

The radiation absorbed dose received by normal tissues was calculated for 1 mCi dose each of [^{18}F]FIBG, no-carrier-added [^{124}I]MIBG and [^{124}I]MIBG prepared by the exchange method. For [^{18}F]FIBG, the tissue uptake levels in mice determined at 1, 2 and 4 hr and expressed on a per organ basis (%ID/organ) were used instead of the current results because of the inclusion of the 4-hr time point in that study (*16*). The results at 1 and 2 hr were essentially identical to those observed in the current study. These data were then used to determine the biological half-life in each tissue, which was assumed to be either monoexponential (liver, spleen, lung, stomach, blood) or infinite (heart, kidney, muscle, adrenals). For [^{124}I]MIBG, the %ID/organ values (1–48 hr) obtained from an earlier study for [^{123}I]MIBG (no-carrier-added as well as exchange preparation) were used (*18*). For the adrenals, where the uptake was fairly constant, an infinite $t_{1/2biol}$ was assumed; for all other tissues it was assumed to be monoexponential. Blood-pool activity was used to calculate whole body levels. The residence times (hr) obtained from these data were used to estimate radiation absorbed dose using the MIRDOSE 2 computer program and the standard human adult model.

Statistical Analyses

A paired t-test with one-sided alternative was used to test the significance of differences for data obtained in the paired-label format. For data comparisons between single- and paired-label experiments, an independent t-test was used. Differences with p values of less than 0.05 were considered significant.

RESULTS

In Vitro Binding Studies

The dose dependence of the binding of [^{18}F]FIBG and [^{125}I]MIBG to SK-N-SH neuroblastoma cells was determined in a paired-label format. As shown in Figure 1, the percent binding of [^{18}F]FIBG remained constant (77%–83%) through the 2–3 log-dose range and was higher than that of [^{125}I]MIBG (67%–71%). The differences were statistically significant ($p < 0.05$) at all doses. The percent binding of each tracer in the paired-label format at 75 nCi and 750 nCi doses was slightly more than the corresponding values from parallel experiments using only one tracer at a time. For [^{18}F]FIBG, the values were 78% ± 2% (paired) and 76% ± 3% (single) at 75 nCi and 83% ± 2% (paired) and 76% ± 3% (single) at 750 nCi. In the case of [^{125}I]MIBG, these values were 67% ± 1% (paired) and 61% ± 4% (single) at 75 nCi and 71% ± 1% (paired) and 60% ± 2% (single) at 750 nCi. Except for [^{18}F]FIBG at 75 nCi, the differences were statistically significant ($p < 0.05$). Nonspecific binding, determined by blocking specific uptake using desipramine, was less than 1% in all cases. At 250 nCi and 500 nCi doses, the percent binding of [^{18}F]FIBG to the SK-N-MC cell line was 2%–3%, in comparison to 1%–2% for [^{125}I]MIBG.

To determine whether [^{18}F]FIBG, like MIBG, is taken up via the uptake-1 mechanism by SK-N-SH cells, binding was performed with cells pretreated with uptake-1 inhibitors as well as with carrier MIBG and FIBG. The results are shown in Figure 2. FIBG, MIBG, desipramine and norepinephrine, all at a concentration of 50 μM, reduced

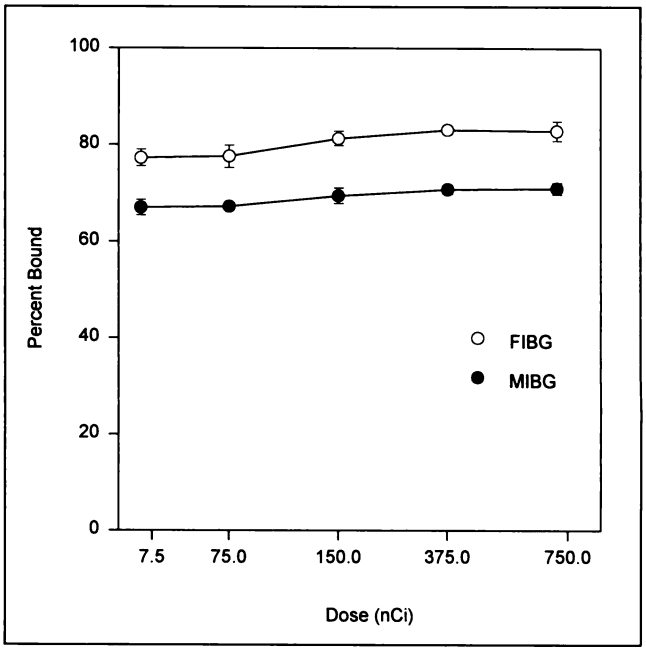

FIGURE 1. Paired-label binding of [^{18}F]FIBG and no-carrier-added [^{125}I]MIBG to SK-N-SH human neuroblastoma cells as a function of the dose.

the uptake to 6%, 6%, 1%, and 10% of control values, respectively. Further, the uptake was energy-dependent, as confirmed by the fact that uptake was reduced to 32% by 1 mM ouabain and to 4% of the control value by conducting the incubation at 4°C (Fig. 3).

Biodistribution in Mice

Tissue distribution of [^{18}F]FIBG in mice was determined in paired-label format by coinjecting no-carrier-added [^{125}I]MIBG in order to obtain a direct comparison of the uptake of the two tracers. At one hour postinjection, uptake of the two tracers was similar in most tissues (Table 1). By 2 hr, however, the liver, spleen, lung, heart and adrenals had significantly ($p < 0.05$) higher uptake of [^{18}F]FIBG. Except for a few tissues, the uptake of both

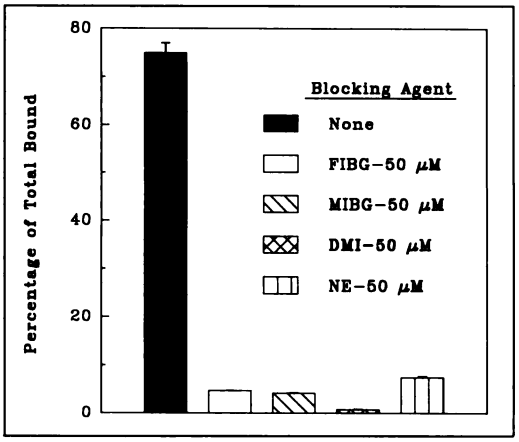

FIGURE 2. Effect of various blocking agents on the binding of [^{18}F]FIBG to SK-N-SH cells.

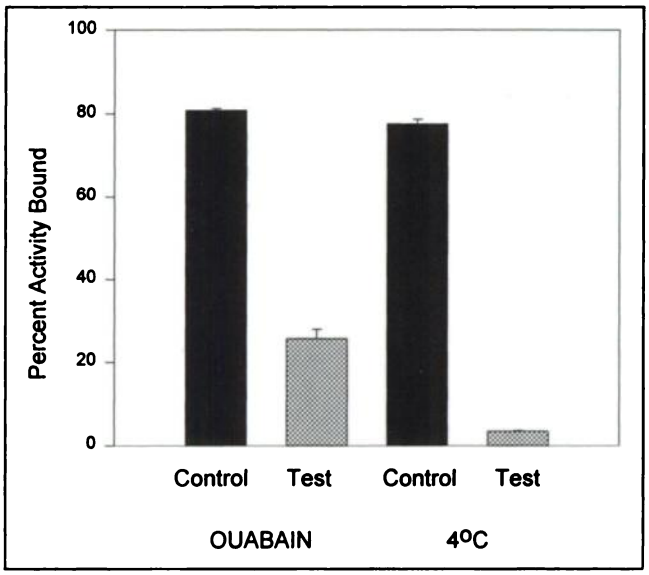

FIGURE 3. Energy-dependence of [^{18}F]FIBG binding to SK-N-SH cells.

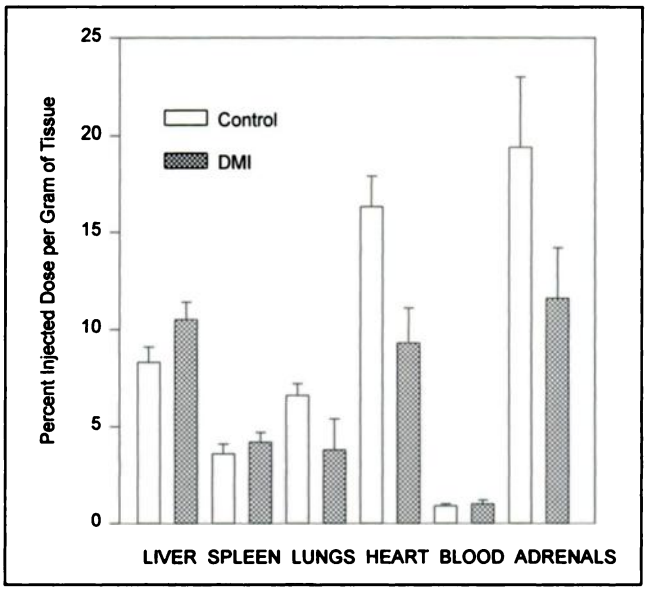

FIGURE 4. Effect of desipramine (DMI) on mouse tissue uptake of [^{18}F]FIBG.

tracers was somewhat lower in the paired-label experiment at 2 hr postinjection; however, these differences were significant in only a few cases. The specificity of [^{18}F]FIBG uptake in mouse tissues was determined by the ability of desipramine to block uptake. As shown in Figure 4, pretreatment of mice with desipramine reduced adrenal and myocardial uptake to 60% and 57% of the control values, respectively, 1 hr after injecting the tracer. The lung uptake also decreased while that of the liver and spleen increased. These differences in uptake were statistically significant ($p < 0.05$).

Radiation Dosimetry

The absorbed dose received by normal tissues was calculated per mCi of administered [^{18}F]FIBG, no-carrier-added [^{124}I]MIBG and [^{124}I]MIBG prepared by the exchange method (Table 2). The adrenals (3.1–3.5 rads) was the critical organ for [^{124}I]MIBG, while the heart (0.2 rad) received the highest dose from [^{18}F]FIBG. The whole body received about 0.1–0.2 rad from [^{124}I]MIBG and 0.04 rad from [^{18}F]FIBG.

TABLE 1
Paired-Label Tissue Distribution of No-Carrier-Added [^{18}F]FIBG and No-Carrier-Added [^{125}I]MIBG in Normal Mice

	1 hr		2 hr			
	[^{18}F]FIBG %ID/g*	[^{125}I]MIBG %ID/g*	[^{18}F]FIBG %ID/g*		[^{125}I]MIBG %ID/g*	
Tissue	Paired	Paired	Paired	Single	Paired	Single
Liver	10.4 ± 0.5	8.4 ± 0.4	12.5 ± 3.3	14.3 ± 1.3	7.4 ± 1.9	8.4 ± 1.1
Spleen	3.5 ± 0.4	3.6 ± 0.4	4.9 ± 0.5	5.4 ± 0.6	4.1 ± 0.3	4.5 ± 0.4
Lungs	7.9 ± 3.6	5.6 ± 2.3	11.0 ± 2.3	10.4 ± 2.0	6.6 ± 1.2	6.8 ± 1.7
Heart	17.2 ± 2.4	18.0 ± 2.7	20.8 ± 3.1	23.8 ± 1.1†	16.2 ± 2.6	18.7 ± 1.7
Kidney	2.6 ± 0.4	2.4 ± 0.4	3.7 ± 0.3	4.2 ± 0.4†	3.0 ± 0.2	3.6 ± 0.8
Stomach	3.7 ± 0.6	4.6 ± 0.6	5.3 ± 1.4	5.2 ± 1.3	5.7 ± 1.2	7.1 ± 2.2
Small intestine	6.4 ± 0.7	7.2 ± 0.7	7.1 ± 1.2	8.2 ± 0.8	8.3 ± 1.2	8.3 ± 1.6
Large intestine	3.7 ± 0.5	4.0 ± 0.4	5.6 ± 0.8	6.4 ± 0.6	6.5 ± 1.5	7.0 ± 1.4
Thyroid	1.9 ± 0.3	2.3 ± 0.5	2.6 ± 0.7	3.8 ± 1.8	4.7 ± 1.2	7.1 ± 1.4†
Muscle	1.7 ± 0.1	1.9 ± 0.2	2.0 ± 0.3	2.4 ± 0.3†	2.0 ± 0.2	2.2 ± 0.4
Bone	1.6 ± 0.1	1.2 ± 0.1	2.2 ± 0.5	1.9 ± 0.3	1.7 ± 0.4	1.6 ± 0.2
Blood	0.9 ± 0.1	0.9 ± 0.1	0.8 ± 0.2	0.7 ± 0.2	1.1 ± 0.3	1.2 ± 0.1
Brain	0.2 ± 0.0	0.1 ± 0.0	0.2 ± 0.1	0.2 ± 0.1	0.2 ± 0.1	0.2 ± 0.0
Adrenals	17.9 ± 3.2	18.2 ± 4.0	20.3 ± 2.5	25.4 ± 4.5†	17.1 ± 3.2	22.0 ± 4.0†

*Percent injected dose per gram of tissue; mean ± s.d. (n = 5).
†Differences between single- and paired-label data are statistically significant ($p < 0.05$).

TABLE 2
Absorbed Dose Estimates (per mCi) in Adults for [^{18}F]FIBG or [^{124}I]MIBG

	Absorbed dose (rads/mCi)		
		[^{124}I]MIBG	
Target organ	[^{18}F]FIBG	No-carrier-added	Exchange
Adrenals	0.09	3.52	3.07
Heart wall	0.16	0.68	0.46
Kidney	0.09	0.56	0.44
Liver	0.14	0.72	0.52
Lungs	0.04	0.21	0.15
Muscle	0.03	0.11	0.10
Spleen	0.05	0.35	0.30
Stomach	0.05	0.42	0.44
Whole body	0.04	0.15	0.13

DISCUSSION

One of the potential advantages of PET is that one could use it to get estimates of radiation dosimetry to assist in the planning of subsequent treatment using a radiotherapeutic agent. Since MIBG has found widespread applications in the clinical management of neuroendocrine tumors, a positron-emitting analog of MIBG might be useful for this purpose. Indeed, [^{124}I]MIBG has been used in a pilot study to estimate dosimetry (*12*); however, lack of ^{124}I availability has impeded progress with this approach.

There are a number of other nuclides available for PET, and ^{18}F is the longest half-life nuclide routinely available at most PET centers. In addition, because of its shorter half-life, the absorbed dose imparted to critical organs from a ^{18}F-labeled MIBG analog could be lower than [^{124}I]MIBG and it should be possible to perform repetitive scanning. This could be of particular value for potential applications in cardiology. In order to obtain a realistic estimate of the expected dosimetry from the therapeutic agent, the pharmacokinetics of the PET tracer should mimic those of the the compound to be used in therapy. Ideally, it should be possible to individually label the MIBG analog with either a positron-emitting nuclide or a therapeutic nuclide. Since fluorine is a bioisostere of aromatic hydrogen, it has been predicted that 4-[^{18}F]fluoro-3-iodobenzylguanidine would be an excellent analog of MIBG for use in PET applications (*20*). Our initial studies (*16*) suggested that this indeed may be the case.

Our first step was to evaluate the nature of the in vitro binding of [^{18}F]FIBG to the SK-N-SH human neuroblastoma cell line. We reported previously that the binding of no-carrier-added [^{131}I]MIBG to SK-N-SH cells remained constant over a 2–3 log activity range, whereas that of [^{131}I]MIBG synthesized by isotopic exchange decreased with increasing doses, indicating that this binding was saturable (*17*). Binding of [^{18}F]FIBG also remained constant over a 100-fold range of doses (*16*), suggesting the lack of impurity or carrier in the preparation that could compete with [^{18}F]FIBG for cell uptake.

In comparing two tracers, paired-label studies (*21*) are of value as both tracers are subjected to identical conditions and each set of experimental conditions can serve as its own control. If one or both tracers are carrier-added, however, such an approach is not possible. The in vitro binding of [^{18}F]FIBG was similar to that of no-carrier-added [^{125}I]MIBG when performed in a paired-label format. Furthermore, the percent of activity bound for each tracer did not decrease when going from a single-label to a paired-label experiment. These results suggest that it is possible to perform paired-label in vitro assays with these tracers. The actual percentage of activity bound for both tracers was 20%–25% higher than reported earlier (*16*), suggesting that the absolute amount bound was dependent on the passage number of this neuroblastoma cell line. Such experiment-to-experiment variation in binding has also been reported by Lashford et al. (*22*). This underscores the need for either doing parallel experiments with a control tracer or, if feasible, using a paired-label format.

In SK-N-SH cells, MIBG is taken up mainly by a neuron-specific, active, uptake-1 process (*23,24*). The tricyclic antidepressant drug desipramine (0.6 μM) has been shown to reduce MIBG uptake to less than 5% of control values (*23*). Desipramine (0.5 μM) also reduced the uptake of meta-[^{211}At]astatobenzylguanidine (MABG) to 11% of control values (*25*). With [^{18}F]FIBG, the uptake was reduced to less than 1% of the control values when the cells were treated with 50 μM desipramine. Norepinephrine, for which MIBG is a functional analog, at 100 μM reduced MIBG uptake to less than 5% of the control values (*23*) and at 10 μM blocked [^{211}At]MABG to 10% of the control values (*25*). At 50 μM, norepinephrine reduced [^{18}F]FIBG uptake to the same degree. These results suggest that [^{18}F]FIBG, like MIBG, is taken up by SK-N-SH cells via an active uptake-1 mechanism. This was further corroborated by the fact that the uptake was also blocked by carrier MIBG. The saturability and specificity of the uptake were confirmed by its blocking with carrier FIBG. The uptake-1 mechanism is energy-dependent (*24*). Ouabain, an ATPase inhibitor, and lower temperature inhibited both MIBG (*24*) and [^{211}At]MABG (*25*) uptake by SK-N-SH cells. FIBG uptake by SK-N-SH cells was also suppressed by these conditions, thereby validating that [^{18}F]FIBG uptake, like that of MIBG, is energy-dependent.

In paired-label tissue distribution measurements performed in mice, the normal tissue uptake of [^{18}F]FIBG was similar to that of [^{125}I]MIBG in most tissues at 1 hr postinjection, and similar to that observed in humans in the absence of neural crest tumors (*26*). Significantly higher uptake of [^{18}F]FIBG was seen, however, at 2 hr in the heart, adrenals, liver and lung. The difference in liver uptake between [^{125}I]MIBG and [^{18}F]FIBG could be due to slight differences in their lipophilicity or due to deiodination. Lipophilicity measurements (*16*) showed that FIBG is slightly more lipophilic than MIBG, although the difference was not statistically significant. Deiodinases in the liver could generate free iodide from both tracers. Only iodine lost from [^{125}I]MIBG, however, could result in altered ac-

tivity levels in the liver, since free iodide is retained more avidly in other tissues such as the gastrointestinal tract and thyroid.

Pharmacological intervention using the uptake-1 inhibitor desipramine reduced myocardial and adrenal uptake of [^{18}F]FIBG substantially (43% and 40% reduction in heart and adrenals, respectively). In comparison, these values for no-carrier-added [^{123}I]MIBG were 51% and 39% for the heart and adrenals, respectively (Vaidyanathan and Zalutsky, unpublished results). Sisson et al. (*27*) reported a 50% decrease (2 hr after tracer administration) in myocardial MIBG uptake in rats pretreated with desipramine, whereas Vallete et al. (*13*) reported a 42% reduction 4 hr after tracer administration. With regard to other halobenzylguanidine analogs, desipramine pretreatment resulted in 33% and 45% decreases of [^{211}At]MABG uptake in mouse heart and adrenals 1 hr postinjection, respectively (*25*). Likewise, a 64% reduction of meta-[^{76}Br]bromobenzylguanidine ([^{76}Br]MBBG) uptake in the rat heart (2 hr postinjection of tracer) was reported by Vallete et al. (*13*). The difference in the reduction of myocardial uptake between [^{123}I]MIBG and [^{76}Br]MBBG by desipramine was attributed to the different lipophilicities of these tracers, thus suggesting that the dependence of neuronal uptake on passive diffusion increased with increasing lipophilicity of the tracer. In comparing the data for [^{76}Br]MBBG, [^{123}I]MIBG, [^{18}F]FIBG and [^{211}At]MABG, one can see that [^{18}F]FIBG and [^{211}At]MABG are consistent with this pattern.

The shorter half-life of ^{18}F in comparison to 4.2 days for ^{124}I is an additional factor that must be considered in evaluating the potential applicability of [^{18}F]FIBG and [^{124}I]MIBG. Because the half-life of ^{124}I is closer to that of ^{131}I, it should be easier to examine organ distribution patterns at longer time points, thereby facilitating dosimetry prediction prior to therapy. This potential limitation of ^{18}F is ameliorated by the fact that the clearance of MIBG from the body is rapid. For example, Lashford et al. (*28*) have reported rapid blood clearance and organ uptake of [^{131}I/^{123}I]MIBG and greater than 50% urinary excretion in the first 8 hr in children with neuroblastoma. Because of the rapid blood clearance observed with MIBG and its analogs, it seems likely that the short half-life of ^{18}F will not be incompatible with imaging neuroendocrine tumors or the myocardium using [^{18}F]FIBG. Indeed, Shulkin et al. (*29*) were able to detect pheochromocytoma in a patient by PET using [^{11}C] hydroxyephedrine. Also, in the scanning of the myocardium with [^{123}I]MIBG, images were obtained typically within 2–4 hr of tracer administration (*30,31*).

An important advantage of [^{18}F]FIBG is that its radiation dosimetry is more favorable than that of [^{124}I]MIBG. The administered doses in a clinical study using [^{124}I]MIBG were only about 0.6 mCi and 1.1 mCi (*12*). Although the rationale for using these dose levels was not discussed, our dosimetry estimates calculated for [^{124}I]MIBG suggest that avoiding excessive normal tissue dose may have been a factor. Because of anticipated dose limitations for [^{124}I]MIBG and imaging problems associated with the high-energy gamma rays emitted by ^{124}I, it might be difficult to obtain useful image and quantification data for extended periods after tracer administration.

Although an approximately twentyfold advantage for [^{18}F]FIBG in critical organ dose would appear to exist, it is important to note that the rapid urinary elimination of this compound would likely result in the bladder being the actual critical organ for this compound. In the current study, bladder doses were not calculated because of difficulties in obtaining realistic cumulative activity levels in the mouse. If one assumes similar urinary excretion of MIBG and [^{18}F]FIBG, then human data obtained with MIBG could be used as an initial estimate of [^{18}F]FIBG bladder dosimetry. The results of Lashford et al. (*28*) suggest that about 20% of the injected dose is excreted in the urine during the first 30 min with cumulative excretion increasing slowly thereafter. If instantaneous bladder uptake of 20% of the injected dose of [^{18}F]FIBG were assumed, then a bladder dose of about 1 rad/mCi would be calculated. This level is comparable to those for other ^{18}F-labeled tracers that have been used clinically (*32,33*). Further studies are planned in normal dogs to obtain a better estimate of the radiation dosimetry of [^{18}F]FIBG.

CONCLUSION

We have demonstrated that [^{18}F]FIBG is taken up by human neuroblastoma cells in vitro by an uptake-1 mechanism similar to that of MIBG. Paired-label tissue distribution experiments in mice indicated nearly identical localization of the two tracers in anticipated normal tissue targets, the adrenals and the heart, and that this uptake could be blocked using desipramine. Taken together, these results suggest that [^{18}F]FIBG could be a useful MIBG analog that may have applications with PET in oncology and cardiology.

ACKNOWLEDGMENTS

The authors thank Ms. Susan Slade and Mr. Phil Welsh for their excellent technical assistance and Ms. Sandra Gatling for preparing the manuscript. This work was supported by National Institutes of Health grant CA 60066 and Department of Energy grant DE-FG05-89ER60789.

REFERENCES

1. Wieland DM, Brown LE, Rogers WL, et al. Myocardial imaging with a radioiodinated norepinephrine storage analog. *J Nucl Med* 1981;22:22–31.
2. Tobes MC, Jacques S Jr, Wieland DM, Sisson JC. Effect of uptake-one inhibitor on the uptake of norepinephrine and metaiodobenzylguanidine. *J Nucl Med* 1985;26:897–907.
3. Wurtman RJ. *Catecholamines.* Boston: Little Brown and Co.; 1966:61–100.
4. Wakasugi S, Wada A, Hasegawa Y, Nakano S, Shibata N. Detection of abnormal cardiac adrenergic neuron activity in adriamycin-induced cardiomyopathy with iodine-125-metaiodobenzylguanidine. *J Nucl Med* 1992;33:208–214.
5. Stanton MS, Tuli MM, Radtke NL. Regional sympathetic denervation after myocardial infarction in humans detected noninvasively using I-123 metaiodobenzylguanidine. *J Am Coll Cardiol* 1988;14:1519–1529.
6. McEwan AJ, Shapiro B, Sisson J, Beierwaltes WH, Ackery DM. Radioiodobenzylguanidine for the scintigraphic location and therapy of adrenergic tumors. *Semin Nucl Med* 1985;15:132–153.

7. McEwan AJ, Wyeth P, Ackery D. Radioiodinated iodobenzylguanidines for diagnosis and therapy. *Appl Radiat Isot* 1986;37:765–775.
8. Wieland DM, Brown LE, Tobes W, et al. Imaging the primate adrenal medulla with [^{123}I] and [^{131}I]meta-iodobenzylguanidine: concise communication. *J Nucl Med* 1981;22:358–364.
9. McGhie AI, Corbett JR, Akers MS, et al. Regional cardiac adrenergic function using I-123 meta-iodobenzylguanidine tomographic imaging after acute myocardial infarction. *Am J Cardiol* 1991;67:236–242.
10. Shulkin BL, Shapiro B, Francis I, Door R, Shew S-W, Sisson JC. Primary extra-adrenal pheochromocytoma positive I-123 MIBG imaging with negative I-131 MIBG imaging. *Clin Nucl Med* 1986;11:851–854.
11. Feine V, Müller-Schauenburg W, Truener J, Klingebid Th. Metaiodobenzylguanidine (MIBG) labeled with ^{123}I/^{131}I in neuroblastoma diagnosis and follow-up treatment with a review of the diagnostic results of the international workshop of pediatric oncology held in Rome, September 1986. *Med Ped Oncol* 1987;15:181–187.
12. Ott RJ, Tait D, Flower MA, Babich JW, Lambrecht RM. Treatment planning for ^{131}I-MIBG radiotherapy of neural crest tumours using ^{124}I-MIBG positron emission. *Br J Radiol* 1992;65:787–791.
13. Valette H, Loc'h C, Mardon K, et al. Bromine-76-metabromobenzylguanidine: a PET radiotracer for mapping sympathetic nerves of the heart. *J Nucl Med* 1993;34:1739–1744.
14. Loc'h C, Mardon K, Valette H, Brutesco C, Merlet P, Syrota A, Maziere B. Preparation and pharmacological characterization of [^{76}Br]-meta-bromobenzylguanidine ([^{76}Br]MBBG). *Nucl Med Biol* 1994;21:49–55.
15. Garg PK, Garg S, Zalutsky MR. Synthesis and preliminary evaluation of para- and meta-[^{18}F]fluorobenzylguanidine. *Nucl Med Biol* 1994;21:97–103.
16. Vaidyanathan G, Affleck DJ, Zalutsky MR. 4-[^{18}F]Fluoro-3-iodo-benzylguanidine, a potential MIBG analog for positron emission tomography. *J Med Chem* 1994;37:3655–3662.
17. Vaidyanathan G, Zalutsky MR. No-carrier-added synthesis of meta-[^{131}I]iodobenzylguanidine. *Appl Radiat Isot* 1993;44:621–628.
18. Vaidyanathan G, Zalutsky MR. No-carrier-added [^{123}I]MIBG: synthesis and preliminary evaluation. *Nucl Med Biol* 1994:in press.
19. Biedler JN, Helson L, Spengler BA. Morphology and growth, tumorigenicity and cytogenetics of human neuroblastoma cells in continuous culture. *Cancer Res* 1973;33:2643–2652.
20. Wieland DM. Radiopharmaceutical Design: the adrenal medulla and its diseases. In: Fritzberg AR, ed. *Radiopharmaceuticals: progress and clinical perspectives*, volume 1. Boca Raton, FL: CRC Press; 1986:117–153.
21. Pressman D, Day ED, Blau M. The use of paired labeling in the determination of tumor-localizing antibodies. *Cancer Res* 1957;17:845–850.
22. Lashford LS, Hancock JP, Kemshead JT. Meta-iodobenzylguanidine (MIBG) uptake and storage in the human neuroblastoma cell line SK-N-BE(2C). *Int J Cancer* 1991;47:105–109.
23. Smets LA, Loesberg C, Janssen M, Metwally EA, Huiskamp R. Active uptake and extravesicular storage of m-iodobenzylguanidine in human neuroblastoma SK-N-SH cells. *Cancer Res* 1989;49:2941–2944.
24. Buck J, Bruchelt G, Girgert R, Treuner J, Niethammer D. Specific uptake of m-[^{125}I]iodobenzylguanidine in the human neuroblastoma cell line SK-N-SH. *Cancer Res* 1985;45:6366–6370.
25. Vaidyanathan G, Strickland DK, Zalutsky MR. Meta-[^{211}At]astatobenzylguanidine: further evaluation of a potential therapeutic agent. *Int J Cancer* 1994;57:908–913.
26. Parisi MT, Sandler ED, Hattner RS. The biodistribution of metaiodobenzylguanidine. *Semin Nucl Med* 1992;22:46–48.
27. Sisson JC, Wieland DM, Sherman P, Mangner TJ, Tobes MC, Jacques S. Metaiodobenzylguanidine as an index of the adrenergic nervous system integrity and function. *J Nucl Med* 1987;28:1620–1624.
28. Lashford LS, Moyes J, Ott R, et al. The biodistribution and pharmacokinetics of meta-iodobenzylguanidine in childhood neuroblastoma. *Eur J Nucl Med* 1988;13:574–577.
29. Shulkin BL, Wieland DM, Schwaiger M, et al. PET scanning with hydroxyephedrine: an approach to the localization of pheochromocytoma. *J Nucl Med* 1992;33:1125–1131.
30. Kline RC, Swanson DP, Wieland DW, Thrall JH, Gross MD, Pitt B, Beierwaltes WH. Myocardial imaging in man with I-123 meta-iodobenzylguanidine. *J Nucl Med* 1981;22:129–132.
31. Merlet P, Valette H, Dubois-Randé J-L, et al. Prognostic value of cardiac metaiodobenzylguanidine imaging in patients with heart failure. *J Nucl Med* 1992;33:471–474.
32. Mejia AA, Nakmura T, Masatoshi I, Hatazawa J, Masaki M, Watanuki S. Estimation of absorbed doses in humans due to intravenous administration of fluorine-18-fluorodeoxyglucose in PET studies. *J Nucl Med* 1991;32:699–706.
33. Goldstein DS, Chang PC, Smith CB, Herscovitch P, Austin SM, Eisenhofer G, Kopin IJ. Dosimetric estimates for clinical positron emission tomographic scanning after injection of [^{18}F]-6-fluorodopamine. *J Nucl Med* 1991;32:102–110.